Calculation of Electron Energy Distribution Functions From Electron Swarm Parameters Using Artificial Neural Network in SF_6 and Argon

S. S. Tezcan, M. Ali Akcayol, Ozgur Cemal Ozerdem, and M. S. Dincer

***Abstract*—This paper proposes an artificial neural network (ANN) to obtain the electron energy distribution functions (EEDFs) in SF_6 and argon from the following: 1) mean energies; 2) the drift velocities; and 3) other related swarm data. In order to obtain the required swarm data, the electron swarm behavior in SF_6 and argon is analyzed over the range of the density-reduced electric field strength E/N from 50 to 800 Td from a Boltzmann equation analysis based on the finite difference method under a steady-state Townsend condition. A comparison between the EEDFs calculated by the Boltzmann equation and by ANN for various values of E/N suggests that the proposed ANN yields good agreement of EEDFs with those of the Boltzmann equation solution results.**

***Index Terms*—Argon, boltzmann equation, neural networks, SF_6.**

I. Introduction

SF_6 is often used in high-voltage equipment because of the following: 1) its high dielectric strength; 2) chemical stabilty and inertness; 3) its thermal stability; and 4) its nontoxicty and nonflammability. However, it is an efficient absorber of the infared radiation and specified as a powerful greenhouse gas. On the other hand, argon has a wide variety of applications, such as the following: 1) gas laser; 2) plasma; 3) arc welding; 4) steel fabrication; 5) heat treatment; 6) electronic manufacturing; and 7) the laboratory studies of plasma, and has gained importance in recent years in pulsed power switching applications because of the following: 1) its low arc inductance; 2) its ability to conduct high currents; and 3) its chemical stability to higher temperatures. Monte Carlo simulations [1], [2] and Boltzmann equation methods [3], [4] have been applied to carry out the theoretical studies of the electron swarm parameters.

In the present paper, the electron drift velocity, mean energy and transverse diffusion coefficient, and ionization and effective ionization coefficients are determined in SF_6 and argon by using a Boltzmann equation method over the range of E/N from 50 to 800 Td. Electron swarm parameters are calculated from the appropriate integrals over the product of a cross section and electron energy distribution function (EEDF).

The relationship between the EEDF and the swarm parameters is the mapping

$$f(\varepsilon) \Rightarrow \begin{matrix} \overline{\alpha}(E/N) \\ W(E/N) \\ \overline{\varepsilon}(E/N) \\ D_T N(E/N) \end{matrix} \tag{1}$$

and to find the reverse mapping, an artificial neural network (ANN) can be designed. The aim of this paper is to propose an ANN to explore the mapping between the electron swarm parameters and EEDFs in SF_6 and argon gases. To the best of our knowledge, such an analysis is lacking in the literature, although the feasibility of using neural computing to obtain cross sections from electron swarm data has been presented before [5] and, also, there are several papers available in the literature discussing numerical optimization procedures to obtain cross sections from electron swarm data [6]–[8]. In order to develop the ANN, electron swarm parameters are calculated in SF_6 and argon over a wide range of the reduced electric field strength E/N from 50 to 800 Td by using the Boltzmann equation method.

II. Boltzmann Equation Analysis

Using the steady-state Townsend method, the distribution function of electron energies for SF_6 and argon have been obtained by a numerical solution of the Boltzmann equation which takes into account a set of electron cross sections. The electron swarm parameters are calculated by a Boltzmann equation method given by [9], and herein expressed explicitly in (2). Q_m, Q_i, and Q_a are the electron cross sections for momentum transfer, ionization, and attachment, respectively. $Q_m^e = Q_m + \sum_j Q_j + Q_i + Q_a$ denotes the effective collision cross section for momentum transfer as the sum of the momentum transfer, inelastic ionization, and attachment cross sections. Δ specifies the energy partition between the primary and secondary electrons after an ionizing collision and equal energy partition is considered with a Δ value of 0.5 in this paper. Q_j and ε_j are the inelastic cross sections and the threshold energies

Manuscript received October 13, 2009; revised February 4, 2010 and April 5, 2010; accepted April 24, 2010. Date of publication May 24, 2010; date of current version September 10, 2010.

S. S. Tezcan and M. S. Dincer are with the Department of Electrical and Electronics Engineering, Gazi University, 06570 Ankara, Turkey (e-mail: stezcan@gazi.edu.tr; sedincer@gazi.edu.tr).

M. Ali Akcayol is with the Department of Computer Engineering, Gazi University, 06570 Ankara, Turkey (e-mail: akcayol@gazi.edu.tr).

O. C. Ozerdem is with the Department of Electrical and Electronics Engineering, Near East University, Nicosia, Cyprus (e-mail: oozerdem@neu.edu.tr).

Digital Object Identifier 10.1109/TPS.2010.2049588

associated with the vibrational $(j=1)$ and the electronic $(j=2)$ excitation. Thus, we have

$$\left(\frac{eE}{N}\right)^2 \frac{d}{d\varepsilon}\left(\frac{\varepsilon}{3Q_m^e}\frac{df}{d\varepsilon}\right)+\left(\frac{eE}{N}\right)\left(\frac{\alpha-\eta}{N}\right)\frac{d}{d\varepsilon}\left(\frac{\varepsilon}{3Q_m^e}f\right)$$
$$+\left(\frac{eE}{N}\right)\left(\frac{\alpha-\eta}{N}\right)\frac{\varepsilon}{3Q_m^e}\frac{df}{d\varepsilon}+\left(\frac{\alpha-\eta}{N}\right)^2\frac{\varepsilon}{3Q_m^e}f$$
$$+\frac{2m}{M}\frac{d}{d\varepsilon}(\varepsilon^2 Q_m f)$$
$$+\sum_j\left((\varepsilon+\varepsilon_j)Q_j(\varepsilon+\varepsilon_j)f(\varepsilon+\varepsilon_j)-\varepsilon Q_j(\varepsilon)f(\varepsilon)\right)$$
$$+\frac{1}{\Delta}\left(\frac{\varepsilon}{\Delta}+\varepsilon_i\right)Q_i\left(\frac{\varepsilon}{\Delta}+\varepsilon_i\right)f\left(\frac{\varepsilon}{\Delta}+\varepsilon_i\right)$$
$$+\frac{1}{1-\Delta}\left(\frac{\varepsilon}{1-\Delta}+\varepsilon_i\right)Q_i\left(\frac{\varepsilon}{1-\Delta}+\varepsilon_i\right)f\left(\frac{\varepsilon}{1-\Delta}+\varepsilon_i\right)$$
$$-\varepsilon Q_i(\varepsilon)f(\varepsilon)-\varepsilon Q_a(\varepsilon)f(\varepsilon)=0 \tag{2}$$

where e is the charge and m is the mass of an electron moving under the influence of the electric field strength E. M is the molecular mass. ε_i is the ionization threshold energy. $\varepsilon=(1/2)\ mV^2$ is the electron kinetic energy where V is the velocity of the electron. *N* is the gas number density. α, η, and $\overline{\alpha}=\alpha-\eta$ are the Townsend primary ionization, attachment, and effective ionization coefficients, respectively.

Equation (2) is solved by a finite difference method under the steady-state Townsend condition. Firstly, a guess value of the effective ionization coefficient α–η (for argon $\eta=0$) is introduced into equation (2) and the corresponding EEDF is obtained; then, from the appropriate integration of the distribution function, the new value of the effective ionization coefficient is found. This calculated value of the effective ionization coefficient is again introduced into the equation to modify the EEDF. This iterative procedure is used until a final convergence for α–η is obtained. The distribution function $f(\varepsilon)$ is normalized so that

$$\int_0^\infty \varepsilon^{0.5} f(\varepsilon)d\varepsilon = 1.$$

The electron swarm coefficients can be derived from the distribution function. Thus, the mean energy is

$$\overline{\varepsilon} = \int_0^\infty \varepsilon^{1.5} f(\varepsilon)d\varepsilon. \tag{3}$$

The electron drift velocity *W* and the density-normalized transverse diffusion coefficient D_TN are given by

$$W = -\frac{e}{3}\frac{E}{N}\left(\frac{2}{m}\right)^{0.5}\int_0^\infty \frac{\varepsilon}{Q_m^e(\varepsilon)}\frac{df(\varepsilon)}{d\varepsilon}d\varepsilon \tag{4.a}$$

$$D_TN = -\frac{1}{3}\left(\frac{2}{m}\right)^{0.5}\int_0^\infty \frac{\varepsilon}{Q_m^e(\varepsilon)}f(\varepsilon)d\varepsilon \tag{4.b}$$

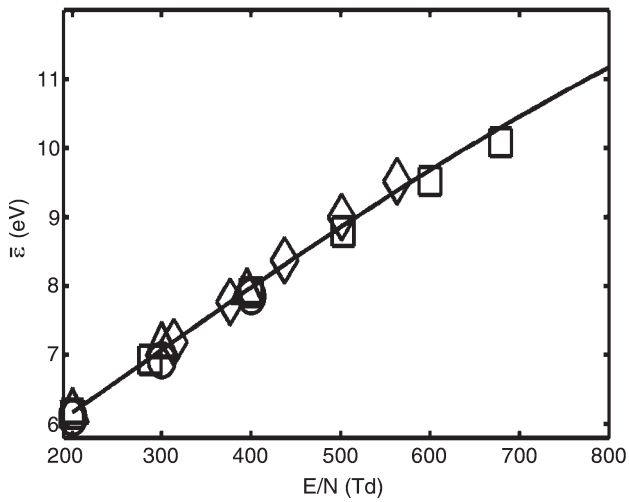

Fig. 1. Electron mean energy in SF_6. Data points: Itoh *et al.* [10]; (□), Benhenni *et al.* [20]; (Δ), Benhenni *et al.* [21]; (O), Dincer [15]; (◇), present results; (—) solid line.

and the Townsend primary ionization coefficient α and attachment coefficient η are calculated from

$$\frac{\alpha}{N} = \left(\frac{2e}{m}\right)^{0.5}\frac{1}{W}\int_{\varepsilon_i}^\infty \varepsilon Q_i(\varepsilon)f(\varepsilon)d\varepsilon \tag{5.a}$$

$$\frac{\eta}{N} = \left(\frac{2e}{m}\right)^{0.5}\frac{1}{W}\int_{\varepsilon_a}^\infty \varepsilon Q_a(\varepsilon)f(\varepsilon)d\varepsilon. \tag{5.b}$$

The electron cross sections of Itoh *et al.* [10], [11] were used for SF_6, whereas those of Hayashi [12] and Yanguas-Gil *et al.* [13] were used for argon. The adopted collision cross section set for SF_6 has been used before and is kept in this paper for the sake of continuity with our previous results [14], [15] although the collision cross section set of Phelps and Van Brunt for SF_6 is also a widely used one [16].

III. Results Obtained From Boltzmann Equation Analysis

In this paper, the effective ionization coefficient, the electron drift velocity, the transverse diffusion coefficient, and the mean energy are determined for SF_6 and argon by using a Boltzmann equation analysis for different E/N values. The swarm coefficients presented in this paper have not been presented in our previous publications, since the form of the Boltzmann equation adopted and the finite difference method employed for the solution of the adopted form have not been used before. The E/N range of the calculations in Ar is from 50 Td to 800 Td while the swarm parameters in SF_6 are calculated from 200 Td to 800 Td since the $E/N_{\rm limit}$ of SF_6 is about 362 Td and for E/N values smaller than the $E/N_{\rm limit}$ values, the discharge will not develop due to the dominant attachment processes. The E/N range selected is sufficient to demonstrate the nonconservative collisions (attachment and ionization).

The electron mean energy calculated in this work for SF_6 is shown in Fig. 1. The values of Benhenni *et al.* [20], [21] and Itoh *et al.* [10] were also included, which show a good agreement with those derived from this paper.

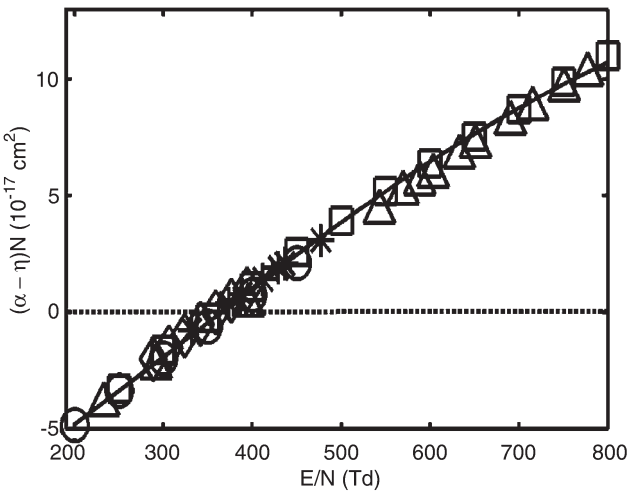

Fig. 2. Effective ionization coefficients $(\alpha\text{-}\eta)/\mathrm{N}$ in SF_6. Data points: Christophorou and Olthoff [17]; (□), Aschwanden [18], [19]; (◊), Pinheiro *et al.* [9]; (O), Itoh *et al.* [11]; (Δ), Dincer *et al.* [14]; (∗), present results; (—) solid line.

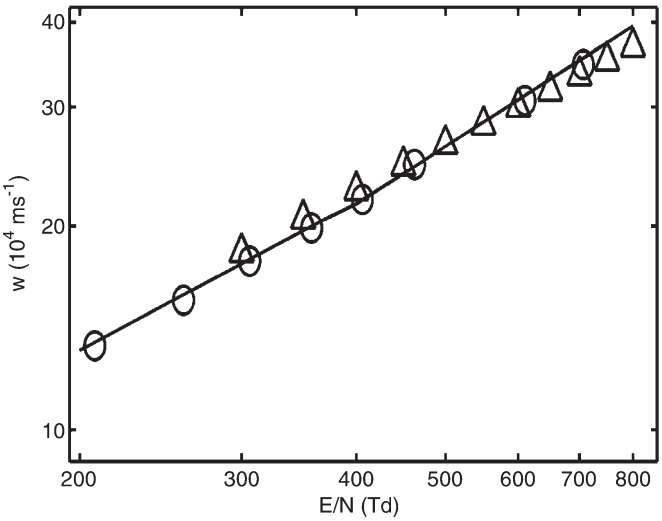

Fig. 3. Electron drift velocity in SF_6. Data points: Christophorou and Olthoff [17]; (Δ), Aschwanden [19]; (O), present results; (—) solid line.

Fig. 2 displays the density-normalized effective ionization coefficients in SF_6 calculated over a range of E/N from 200 to 800 Td. It can be seen from this figure that at the limiting E/N (about 362 Td), the effective ionization coefficient is almost zero, since ionizing collisions are balanced by attaching collisions, and for E/N values smaller than the E/N_{limit}, attachment processes become dominant, yielding negative values for the effective ionization coefficient as E/N is decreased and; on the other hand, for E/N values above the E/N_{limit}, the effective ionization coefficient increases with increasing E/N where the ionization collisions become dominant and the effect of the attachment processes is not significant. There is a good agreement with the results of Aschwanden [18], [19] and Dincer *et al.* [14] for low E/N values, and with those of Christophorou and Olthoff [17] over all the E/N range covered in the present study.

Fig. 3 shows the electron drift velocities as a function of the E/N range from 200 to 800 Td for SF_6. The present electron drift velocities are in reasonable agreement with those reported in the literature [17], [19] over the lower E/N range; however, the agreement becomes poor in the higher E/N range for $E/N > 400$ Td.

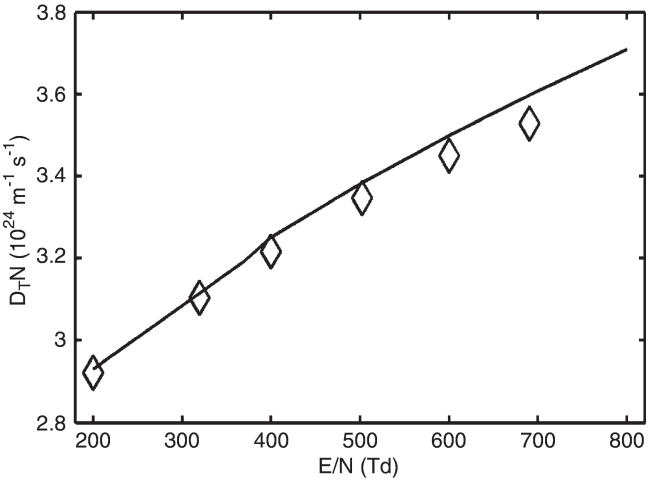

Fig. 4. Transverse diffusion coefficient in SF_6. Itoh *et al.* [11]; (◊), present results; (—) solid line.

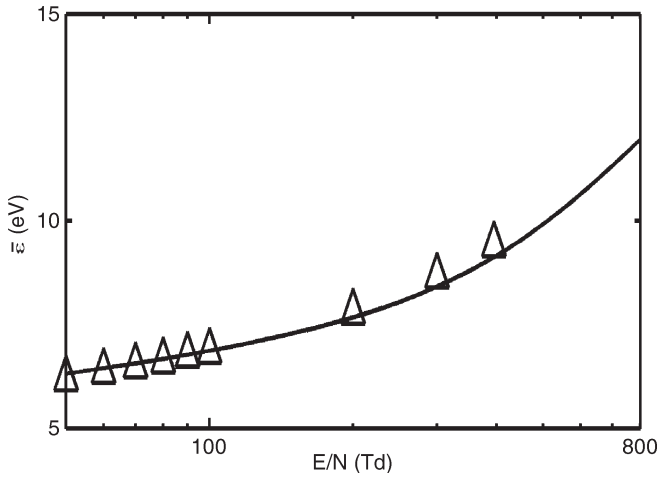

Fig. 5. Electron mean energy in argon. Benhenni *et al.* [20]; (Δ), present results; (—) solid line.

Fig. 4 shows the density-normalized transverse diffusion coefficient $\mathrm{D_TN}$ for pure SF_6 as a function of E/N from 200 to 800 Td. The results of Itoh *et al.* [11] for the transverse diffusion coefficient are also plotted for comparison, and there is a good agreement for $E/N < 400$ Td.

The electron mean energy calculated in this paper for argon is shown in Fig. 5. The values of Benhenni *et al.* [20] are in a good agreement with those derived from this work, particularly for $E/N < 200$ Td.

Fig. 6 displays the density-normalized ionization coefficients in argon as a function of E/N. The results of Phelps and Petrovic [22], Puech and Torchin [23], and Yanguas-Gil *et al.* [13] are also plotted in this figure with reasonable agreement.

Fig. 7 shows the electron drift velocities as a function of the E/N for argon. The present electron drift velocities are in very good agreement with those reported by Raju [24], and there is a reasonable agreement with the results of Jovanovic *et al.* [29].

The comparison of the calculated parameters with those of measurements and with those of exact solutions presented in the

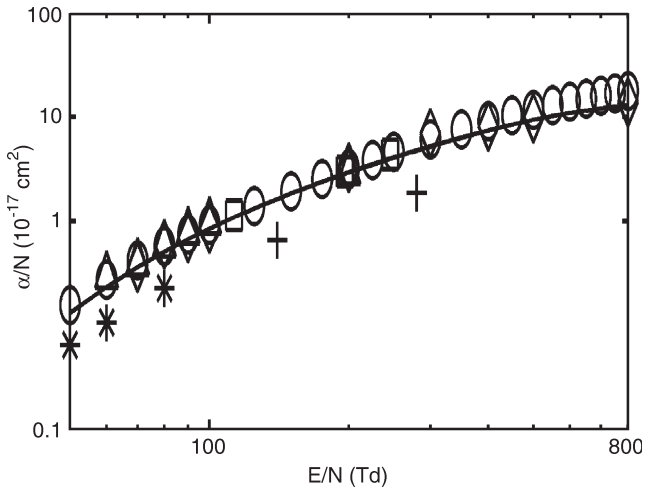

Fig. 6. Ionization coefficients α/N in argon. Data points: Phelps and Petrovic [22]; (O), Puech and Torchin [23]; (Δ), Yanguas-Gil *et al.* [13]; ($\Box$), Maric *et al.* [26]; ($\Diamond$), Abdulla *et al.* [27]; ($*$), Sakai *et al.* [28]; ($+$), present results; ($-$) solid line.

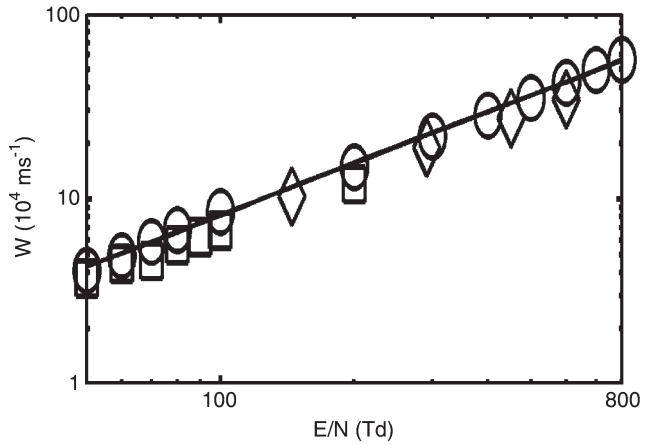

Fig. 7. Electron drift velocity in argon. Data points: Raju [24]; (O), Kucukarpaci and Lucas [25]; ($\Diamond$), Jovanovic *et al.* [29]; ($\Box$), present results; ($-$) solid line.

related figures indicate a reasonable agreement over the lower E/N range; however, deviations from the measurements and exact solutions are observed in our calculations for the high-E/N range, since the Boltzmann equation method used is a two-term approximation with limited accuracy [30].

IV. Artificial Neural Network

The aim of this paper is to propose an ANN to explore mappings between the electron swarm parameters and the EEDFs for SF_6 and argon.

ANNs are computational networks which attempt to simulate the networks of neurons of the biological central nervous system [31]. ANNs have the ability to identify and classify complex relationships that are nonlinear and result from large mathematical models. The main feature of an ANN is the ability to achieve complicated input-output mappings through a learning process, without explicit programming. ANNs have been already used in theoretical studies related to electronegative gases in the literature [32], [33].

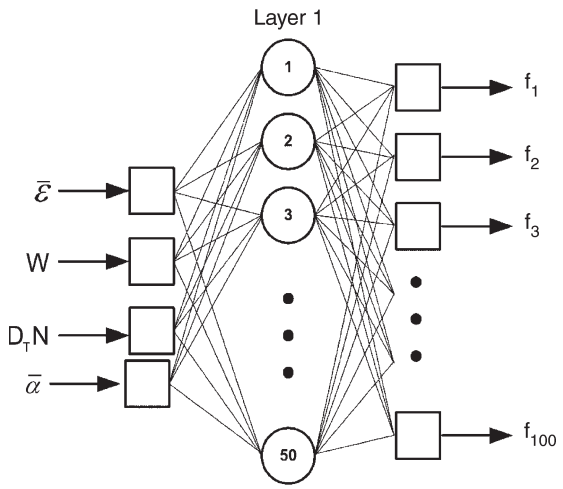

Fig. 8. Schematic diagram of the ANN used in this study.

The ANN is a network of computing units (neurons). Knowledge is encoded into the network through the strength of the connections between different neurons, called weights, and layers that work in parallel. The system learns through a process of determining the number of neurons and adjusting the weights for the connections based upon training data. A multilayer feedforward neural network (MLFF) consists of the following: 1) an input layer; 2) one or more hidden layers; 3) and an output layer. Inputs are fed simultaneously into the neurons making up the input layer. These inputs pass through the input layer and are then weighted and fed simultaneously to a second layer of neurons, known as the hidden layer. The outputs of the hidden layer can be input to another hidden layer, and so on. The neurons of the output layer provide the output variables.

The ANN employed in this paper consists of an input layer with four neurons and an output layer with 100 neurons and one hidden layer with 50 neurons as shown in Fig. 8. The four neurons at the input layer represent the following: 1) mean energy; 2) drift velocity; 3) density-normalized transverse diffusion; and 4) effective ionization/ionization coefficients (the effective ionization for SF_6 and only the ionization coefficient for argon). 100 neurons at the output layer represent the data points obtained from the EEDF at a given E/N.

The *j*th neuron at the output layer is connected to the *i*th neuron in the previous layer via the weight w_{ij}. The output of neuron *j* can be written as

$$o_j = Y\left(\sum_i (w_{ij} o_i)\right) \tag{6}$$

where, i is the neuron in the previous layer, w is the weight of the connection, o is the output of the neuron, and Y is the activation function. In this paper, the sigmoid function is selected as the activation function with the parameters as shown

$$Y(x) = \frac{1}{1 + e^{-4(x-0.5)}} \tag{7}$$

and the sum is over all neurons in the adjacent layer. In this paper, the Generalized Delta Rule (GDR) is used to train the ANN. According to the difference between the produced and target outputs, the weights of the network are adjusted to

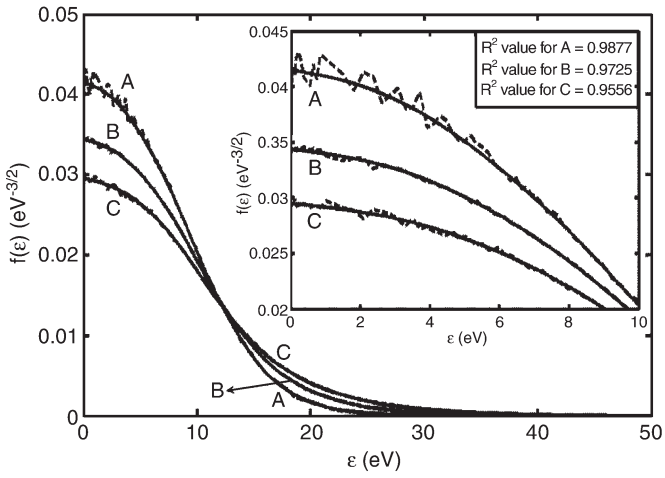

Fig. 9. EEDF in argon: (A) 300 Td. (B) 500 Td. (C) 700 Td. (Solid line: calculated using Boltzmann Equation method, broken line: predicted using ANN).

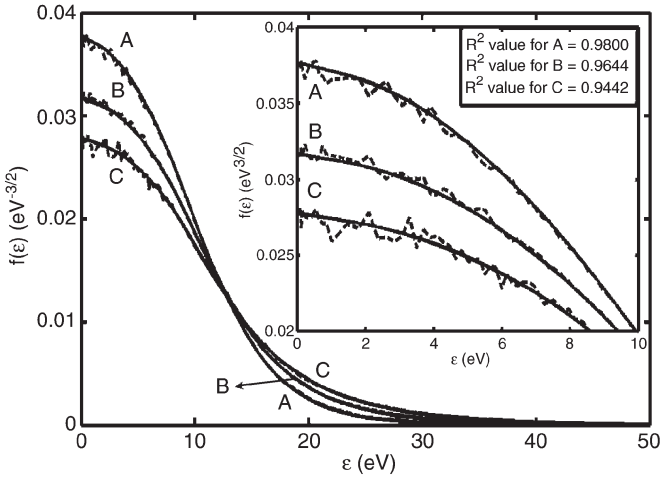

Fig. 10. EEDF in argon: (A) 400 Td. (B) 600 Td. (C) 800 Td. (Solid line: calculated using Boltzmann Equation method, broken line: predicted using ANN).

reduce the output error. The error at the output neuron can be expressed as

$$E = \frac{1}{2}(d_i - o_i)^2. \tag{8}$$

Here, $\mathrm{d_i}$ is the desired output of neuron *i*. The weight $\mathrm{w_{ij}}$ is updated iteratively to minimize *E* for the training data

$$\Delta w_{ij} = \in \delta_i o_j \tag{9}$$

where $\in$ is an adaptation gain. The compution of δ_i is based on whether neuron *i* is in the output layer. If neuron *i* is one of the output neurons, then

$$\delta_i = (d_i - o_i)o_i(1 - o_i). \tag{10}$$

If neuron *i* is not in the output layer, then

$$\delta_i = o_i(1 - o_i)\sum_j w_{ij}\delta_j. \tag{11}$$

After the training of the neural network, it produces an accurate output for a given input data.

The four neurons in the input layer represent the following: 1) mean energy; 2) drift velocity; 3) density-normalized transverse diffusion coefficient; and 4) effective ionization coefficient/ionization coefficient (effective ionization coefficient for SF_6, ionization coefficient for argon) which are calculated at a given E/N by the Boltzmann procedure defined in this paper. The output layer represents the 100 data points sampled from the EEDF, directly obtained from the Boltzmann procedure at a given E/N. Therefore, the input-output pair is the related swarm parameter-EEDF data at a given E/N for the respective gases. Over the E/N range of the present paper, 102 input-output pairs are considered at various E/N values and out of them, 82 input-output pairs are used to train the ANN while the remaining 20 input-output pairs are used for testing the ANN.

Graphs for EEDF in SF_6 and argon are shown in Figs. 9–17. Figs. 9–11 correspond to the results of the learning procedure in argon, while Figs. 12 and 13 present the tested EEDFs in argon for the given E/N values. Similarly, Figs. 14 and 15 correspond

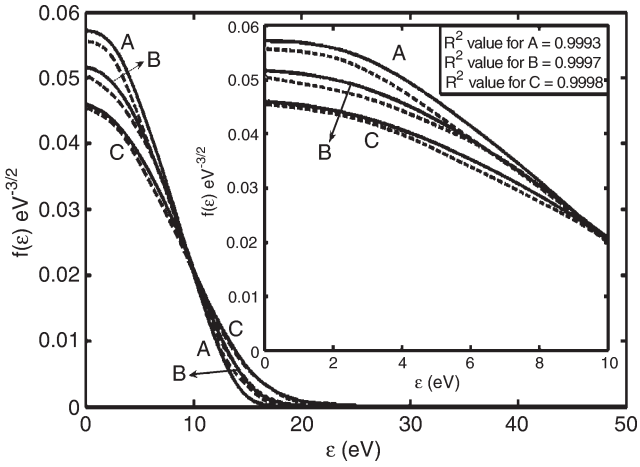

Fig. 11. EEDF in argon: (A) 50 Td. (B) 100 Td. (C) 200 Td. (Solid line: calculated using Boltzmann Equation method, broken line: predicted using ANN).

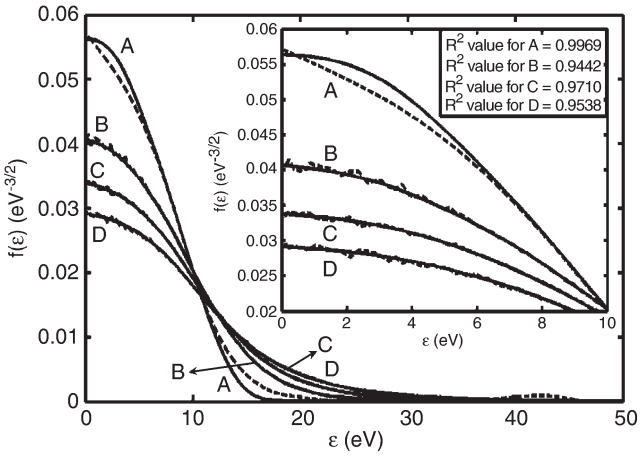

Fig. 12. EEDF in argon: (A) 55 Td. (B) 320 Td. (C) 520 Td. (D) 720 Td. (Solid line: calculated using Boltzmann Equation method, broken line: predicted using ANN).

to the results of the learning procedure in SF_6, while Figs. 16 and 17 present related EEDFs tested by ANN in SF_6 for the given E/N values. In all these figures, in order to compare

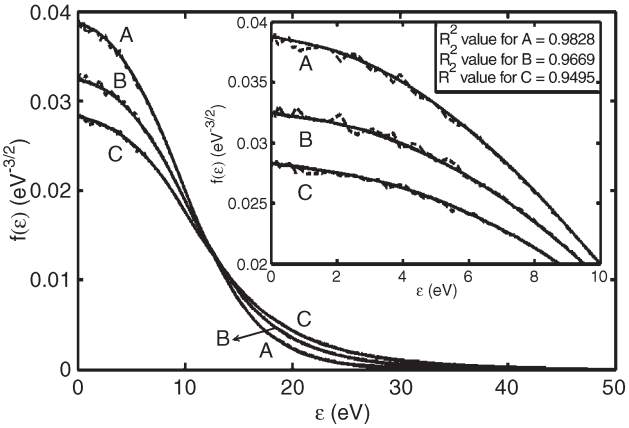

Fig. 13. EEDF in argon: (A) 370 Td. (B) 570 Td. (C) 770 Td. (Solid line: calculated using Boltzmann Equation method, broken line: predicted using ANN).

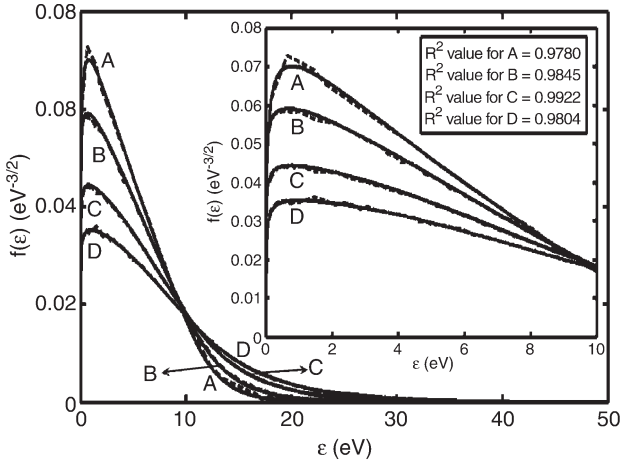

Fig. 14. EEDF in SF_6: (A) 200 Td. (B) 300 Td. (C) 500 Td. (D) 700 Td. (Solid line: calculated using Boltzmann Equation method, broken line: predicted using ANN).

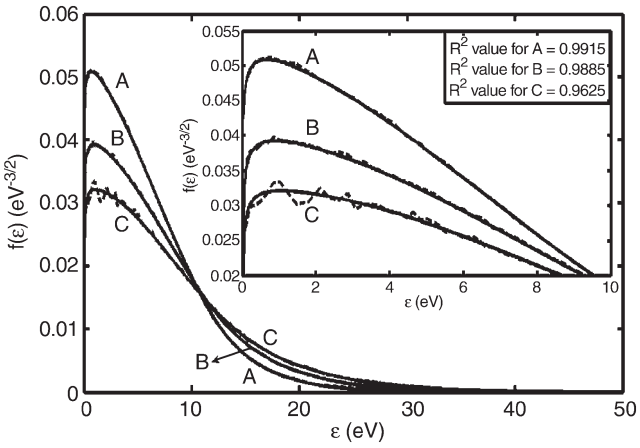

Fig. 15. EEDF in SF_6: (A) 400 Td. (B) 600 Td. (C) 800 Td. (Solid line: calculated using Boltzmann Equation method, broken line: predicted using ANN).

the predicted EEDFs with those from the Boltzmann equation results, the predicted EEDFs are shown by the broken lines. However, since the predicted ANN results of EEDFs are in very good agreement with those of the Boltzmann equation results, the broken lines almost coincide with the solid lines of the Boltzmann equation results. Therefore, for the sake of clarity, in the lower electron energy range, the predicted ANN EEDFs

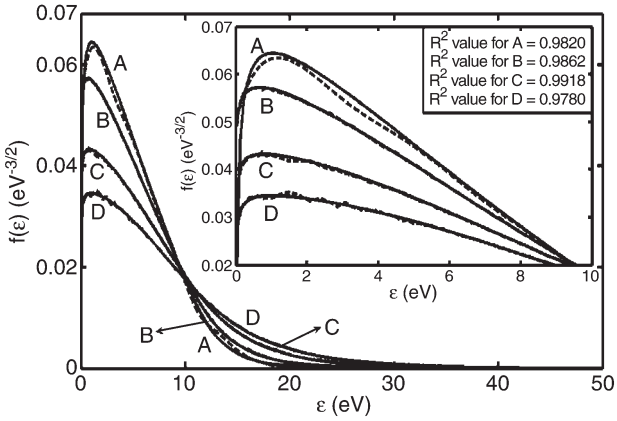

Fig. 16. EEDF in SF_6: (A) 220 Td. (B) 320 Td. (C) 520 Td. (D) 720 Td. (Solid line: calculated using Boltzmann Equation method, broken line: predicted using ANN).

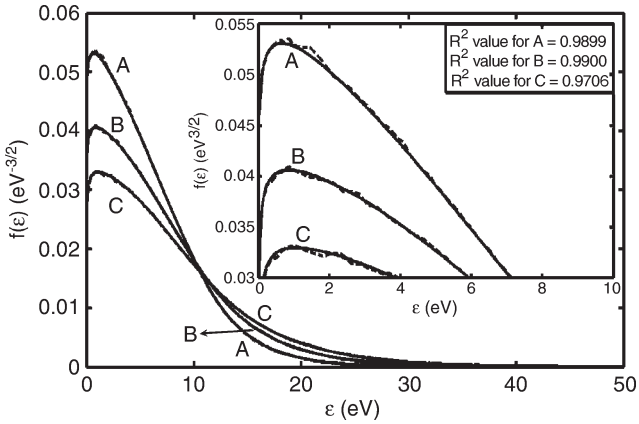

Fig. 17. EEDF in SF_6: (A) 370 Td. (B) 570 Td. (C) 770 Td. (Solid line: calculated using Boltzmann Equation method, broken line: predicted using ANN).

are also compared separately with those from the Boltzmann solution in all these figures. The observed agreement is also supported by the R^2 values, namely, the correlation coefficients, which are also shown in the respective figure. The predicted ANN EEDFs are directly compared with those from the Boltzmann code since the ANN during the learning procedure samples exact data points of the EEDF obtained from the Boltzmann code. The oscillations observed over the low-electron-energy range of the EEDFs have no physical origin and can be suppressed by increasing the number of data points sampled from the corresponding EEDFs which are obtained directly from the Boltzmann procedure. The removal of the oscillations observed over the low electron energy range of the EEDFs is demonstrated in Fig. 11 at 50, 100, and 200 Td for argon, where the number of sampled data points are 150, represented by 150 output neurons. A similar response is also presented for SF_6 at E/N of 200 Td, and is given in Fig. 14.

The Boltzmann procedure adopted for benchmarking in the present paper is a two-term approach and the solution is carried out by employing a finite difference method with the observed CPU times in the order of tens of minutes, depending on the initial values of the iterative procedure at a given E/N to obtain the required EEDFs. However, the learning procedure of the ANN yields CPU times of a few seconds and the ANN EEDF

TABLE I
ANN CPU TIMES

ARGON		SF_6	
E/N (Td)	CPU time (s)	E/N (Td)	CPU time (s)
50	0.0156	200	0.0625
100	0.0155	300	0.0156
200	0.0157	350	0.0158
300	0.0161	400	0.0157
400	0.0158	450	0.0159
500	0.0159	500	0.0161
600	0.0160	600	0.0160
700	0.0162	700	0.0312
800	0.0158	800	0.0320

results at a given E/N can be achieved with CPU times of fractions of seconds as given in Table I.

In Table I, each entry of the CPU time is the arithmetic mean of ten runs for the respective gases at a given E/N. The CPU measurements are carried out in MATLAB R2008b on an AMD Athlon 64 Processor 3200+ 2.00 GHz, with 1.00-GB RAM and 2-MB Cache Memory.

The ANN procedure is faster than the conventional techniques regardless of the complexity of the problem. Furthermore, ANNs overcome the limitations of the conventional methods by extracting the desired information by using the sufficient input-output data. The multiterm solution of the Boltzmann transport equation and Monte Carlo simulations yields exact results of the swarm parameters [34]. However, the CPU times of such methods are expensive and can become prohibitively long for the nonconservative cases [15], although the nonconservative transport is an important subject of kinetic phenomena in charged particle transport in gases [35]. Provided that sufficient data are available from exact solutions for input-output pairs of the related swarm parameter-EEDFs, then the ANN can be trained to yield EEDFs over a wide E/N range with very short inexpensive CPU times. Furthermore, lookup tables can be constructed from the theoretical and experimental swarm data available in the literature to provide input-output pairs in the electronegative gases for electron transport in combined electric and magnetic fields [36] in order to predict ANN EEDFs for various B/N and several angles between the combined fields over a wide E/N range with very short CPU times, yielding important information on EEDFs in such complex models.

V. CONCLUSION

The use of an ANN for obtaining EEDFs in SF_6 and argon from the respective electron swarm parameters has been explored. The proposed ANN inputs are the electron swarm parameters, namely: 1) electron drift velocity; 2) mean energy; 3) density-normalized transverse diffusion coefficient; and 4) effective ionization coefficient/ ionization coefficient, while the output is the EEDF. In order to train and test the ANN, Boltzmann equation calculation results are used. The proposed ANN is a multilayer feedforward backpropagation neural network having one input, one hidden, and one output layer. The predicted EEDFs using the proposed ANN algorithm are found to be in good agreement with the results obtained from the Boltzmann equation procedure.

REFERENCES

[1] M. S. Dincer, H. R. Hiziroğlu, and S. Bektas, "The behaviour of the $N_2 + SF_6$ gas subjected to orthogonal electric and magnetic fields," *IEEE Trans. Dielectr. Elect. Insul.*, vol. 13, no. 2, pp. 257–263, Apr. 2006.

[2] M. S. Dincer and H. R. Hiziroglu, "Limiting equivalent electric field response in $Ar + SF_6$ subjected to orthogonal electric and magnetic fields," *IEEE Trans. Dielectr. Elect. Insul.*, vol. 9, no. 3, pp. 428–432, Jun. 2002.

[3] H. Itoh, M. Kawaguchi, K. Satoh, Y. Miura, Y. Nakao, and H. Tagashira, "Development of electron swarms in SF_6," *J. Phys. D, Appl. Phys.*, vol. 23, no. 3, pp. 299–303, Mar. 1990.

[4] C. M. Ferreira and J. Loureiro, "Electron kinetics in atomic and molecular plasmas," *Plasma Sources Sci. Technol.*, vol. 9, no. 4, pp. 528–540, Nov. 2000.

[5] W. L. Morgan, "The feasibility of using neural networks to obtain cross sections from electron swarm data," *IEEE Trans. Plasma Sci.*, vol. 19, no. 2, pp. 250–255, Apr. 1991.

[6] K. Yoshida, S. Goto, H. Tagashira, C. Winstead, B. V. McKoy, and W. L. Morgan, "Electron transport properties and collision cross sections in C_2F_4," *J. Appl. Phys.*, vol. 91, no. 5, p. 2637, Mar. 2002.

[7] N. Bulatovic, S. Sakadzic, and Z. L. Petrovic, "A test of vibrational excitation cross section in nitrogen by application of genetic algorithm," in *Proc. XIX SPIG*, 1998, pp. 191–194.

[8] W. L. Morgan, "Test of numerical optimization algorithm for obtaining cross sections for multiple collision processes from electron swarm data," *J. Phys. D, Appl. Phys.*, vol. 26, no. 2, pp. 209–214, Feb. 1993.

[9] M. J. Pinheiro and J. Loureiro, "Effective ionization coefficients and electron drift velocities in gas mixtures of SF_6 with He, Xe, CO_2 and N_2 from Boltzmann analysis," *J. Phys. D, Appl. Phys.*, vol. 35, no. 23, pp. 3077–3084, Dec. 2002.

[10] H. Itoh, Y. Miura, N. Ikuta, Y. Nakao, and H. Tagashira, "Electron swarm development in SF_6.I. Boltzmann equation analysis," *J. Phys. D, Appl. Phys.*, vol. 21, no. 6, pp. 922–930, Jun. 1988.

[11] H. Itoh, T. Matsumura, K. Satoh, H. Date, Y. Nakao, and H. Tagashira, "Electron transport coefficients in SF_6," *J. Phys. D. Appl. Phys.*, vol. 26, no. 11, pp. 1975–1979, Nov. 1993.

[12] M. Hayashi, Bibliography of Electron and Photon Cross Sections with Atoms and Molecules Published in the 20th Century—Argon, National Institute for Fusion Science NIFS Data 072, Jan. 2003. [Online]. Available: http://jila.colorado.edu/~avp/collision_data/electronneutral/hayashi.txt

[13] A. Yanguas-Gil, J. Cotrino, and L. L. Alves, "An update of argon inelastic cross sections for plasma discharges," *J. Phys. D, Appl. Phys.*, vol. 38, no. 10, pp. 1588–1598, May 2005.

[14] M. S. Dincer, O. C. Ozerdem, and S. Bektas, "Effective ionization coefficients and transport parameters in ultradilute $SF_6 + N_2$ Mixtures," *IEEE Trans. Plasma Sci.*, vol. 35, no. 5, pp. 1210–1214, Oct. 2007.

[15] M. S. Dincer, "Simulation of electron swarms in SF_6 in uniform $E \times B$ fields," *J. Phys. D, Appl. Phys.*, vol. 26, no. 9, pp. 1427–1431, Sep. 1993.

[16] A. V. Phelps and R. J. Van Brunt, "Electron-transport, ionization, attachment, and dissociation coefficients in SF_6 and its mixtures," *J. Appl. Phys.*, vol. 64, no. 9, pp. 4269–4277, Nov. 1988.

[17] L. G. Christophorou and J. K. Olthoff, "Electron interactions with SF_6," *J. Phys. Chem. Ref. Data*, vol. 29, no. 3, pp. 267–330, May 2000.

[18] T. H. Aschwanden, Ph.D. thesis, Swiss Federal Inst. Technol. (ETH), Zurich, Switzerland, 1985.

[19] T. H. Aschwanden, "Swarm parameters in SF_6 and SF_6/N_2 mixtures determined from a time resolved discharge study," in *Gaseous Dielectrics IV*, L. G. Christophorou and M. O. Pace, Eds. New York: Pergamon, 1984, pp. 24–32.

[20] M. Benhenni, J. de Urquijo, M. Yousfi, J. L. Hernandez-Avila, N. Merbahi, G. Hinojosa, and O. Eichwald, "Measured and calculated SF_6^- collision and swarm ion transport data in $SF_6 - Ar$ and $SF_6 - Xe$ mixtures," *Phys. Rev. E, Stat. Phys. Plasmas Fluids Relat. Interdiscip. Top.*, vol. 71, no. 3, p. 036 405, Mar. 2005.

[21] M. Benhenni, M. Yousfi, J. de Urquijo, and A. Hennad, "Transport properties of SF_6^- in SF_6-Ne, SF_6-N_2 and SF_6-O_2 mixtures," *J. Phys. D, Appl. Phys.*, vol. 42, no. 12, p. 125 203, Jun. 2009.

[22] A. V. Phelps and Z. L. Petrovic, "Cold-cathode discharges and breakdown in argon: Surface and gas phase production of secondary electrons," *Plasma Sources Sci. Technol.*, vol. 8, no. 3, pp. R21–R44, Aug. 1999.

[23] V. Puech and L. Torchin, "Collision cross sections and electron swarm parameters in argon," *J. Phys. D, Appl. Phys.*, vol. 19, no. 12, pp. 2309–2323, Dec. 1986.

[24] G. G. Raju, *Gaseous Electronics: Theory and Practice*. Boca Raton, FL: CRC Press, 2006, pp. 341–350.

[25] H. N. Kucukarpaci and J. Lucas, "Electron swarm parameters in argon and krypton," *J. Phys. D, Appl. Phys.*, vol. 14, no. 11, p. 14, Nov. 1981.

[26] D. Maric, M. Radmilovic-Radenovic, and Z. L. Petrovic, "On parametrization and mixture laws for electron ionization coefficients," *Eur. Phys. J. D*, vol. 35, no. 2, pp. 313–321, Aug. 2005.
[27] R. R. Abdulla, J. Dutton, and A. W. Williams, "Collision cross sections and electron swarm parameters in argon," in *Proc. 15th ICPIG (Minsk)*, 1981, pp. 367–368.
[28] Y. Sakai, H. Tagashira, and S. Sakamoto, "The development of electron avalanches in argon at high E/N values: I. Monte Carlo simulation," *J. Phys. D, Appl. Phys.*, vol. 10, no. 7, pp. 1035–1049, May 1977.
[29] J. V. Jovanovic, E. Basurto, O. Sasic, J. L. Hernandez-Avila, Z. L. Petrovic, and J. de Urquijo, "Electron impact ionization and transport in nitrogen-argon mixtures," in *Proc. 28th ICPIG*, Jul. 15–20, 2007.
[30] R. D. White, R. E. Robson, B. Schmidt, and M. A. Morrison, "Is the classical two-term approximation of electron kinetic theory satisfactory for swarms and plasmas?," *J. Phys. D, Appl. Phys.*, vol. 36, no. 24, pp. 3125–3131, May 2003.
[31] D. Graupe, *Principles of Artificial Neural Networks*., 2nd ed. London, U.K.: World Scientific, 2007, ch. 1.
[32] M. A. Akcayol, H. R. Hızıroğlu, and M. S. Dinçer, "Determination of the response of $Ar + SF_6$ to crossed electric and magnetic fields using an artificial neural network," in *Conf. Rec. IEEE Int. Conf. Elect. Insul. Dielectr. Phenom.*, 2007, pp. 14–17.
[33] S. S. Tezcan, M. S. Dincer, and H. R. Hiziroglu, "Prediction of breakdown voltages in $N_2 + SF_6$ gas mixtures," in *Conf. Rec. IEEE Int. Conf. Elect. Insul. Dielectr. Phenom.*, 2006, pp. 222–225.
[34] S. Dujko, R. D. White, and Z. L. Petrovic, "Monte Carlo studies of non-conservative electron transport in the steady-state townsend experiment," *J. Phys. D, Appl. Phys.*, vol. 41, no. 24, p. 245 205, Dec. 2008.
[35] Z. L. Petrovic, M. Suvakov, Z. Nikitovic, S. Dujko, O. Sasic, J. Jovanovic, G. Malovic, and V. Stojanovic, "Kinetic phenomena in charged particle transport in gases, swarm parameters and their application in plasma modeling," *Plasma Sources Sci. Technol.*, vol. 16, no. 1, pp. S1–S12, Feb. 2007.
[36] Z. L. Petrovic, S. Dujko, D. Maric, G. Malovic, Z. Nikitovic, O. Sasic, J. Jovanovic, V. Stojanovic, and M. Radmilovic-Radenovic, "Measurement and interpretation of swarm parameters and their application in plasma modeling," *J. Phys. D, Appl. Phys.*, vol. 42, no. 19, p. 194 002, Oct. 2009.

S. S. Tezcan was born in Iskenderun, Turkey, on November 5, 1979. He received the B.Sc. degree in electrical engineering from the Yıldız Technical University, Istanbul, Turkey, in 2001, the M.Sc. degree in electrical engineering from the Gazi University, Ankara, Turkey, in 2004.

He is currently with the Department of Electrical and Electronics Engineering, Gazi University, as a Research Assistant. His field of interest is in the field of high-voltage engineering, gaseous electronics and neural networks.

M. Ali Akcayol received the B.S. degree in electronics and computer education from the Gazi University, Ankara, Turkey, in 1993 and 1998, respectively, and the M.Sc. and Ph.D. degrees from the Institute of Science and Technology at the Gazi University, Ankara, Turkey, in 2001.

He is currently teaching computer engineering at the Faculty of Engineering, Gazi University. His research interests include intelligent control, fuzzy logic, neural networks, neuro-fuzzy, genetic algorithm, and mobile wireless systems.

Ozgur Cemal Ozerdem was born in Ankara, Turkey, on November 11, 1967. He received the B.S. and M.S. degrees in electrical and electronic engineering from the Eastern Mediterranean University, Gazimagusa, Cyprus, in 1992 and 1994, respectively, and the Ph.D. degree from the Near East University, Nicosia, Cyprus, in 2005.

He is currently with the Department of Electrical and Electronics Engineering, Near East University, as an Assistant Professor. His field of interest is in power engineering.

M. S. Dincer was born in Ankara, Turkey, in 1952. He received the B.Sc. degree in electrical engineering from the Gazi University, Ankara, in 1975, the M.Sc. degree in electrical engineering from the Middle East Technical University, Ankara, in 1980, and the Ph.D. degree in electrical engineering from the University of Windsor, Windsor, ON, Canada, in 1985.

He is currently a Professor of electrical engineering with the Gazi University, and he also performs consultancy services in the field of high-voltage engineering and gas-insulated systems. His research activities are in the field of high-voltage engineering and gas-insulated systems.